

# Molecular Statics Simulation in Aluminum

Murat Durandurdu

Thesis submitted to the faculty of the  
Virginia Polytechnic Institute and State University  
in partial fulfillment of the requirements for the degree of  
Master of Science

in

Materials Science and Engineering

©Murat Durandurdu and VPI & SU 1999

Approved:

---

Dr. Diana Farkas, Chairperson

---

Dr. William T. Reynolds

---

Dr. Herve Marand

June 1999

Blacksburg, Virginia

KEYWORDS: Dislocations, Cracks, Ductility, Atomistic Simulation, Fracture, Twinning

# Molecular Statics Simulation in Aluminum

Murat Durandurdu

Materials Science and Engineering Department  
Virginia Polytechnic Institute and State University  
Blacksburg, VA 24061

## Abstract

Effects of dislocation emission from a mode I crack and of pinning distances on the behavior of the crack and on fracture toughness in aluminum were studied by using the Molecular Statics Technique with atomic interactions described in terms of the Embedded Atom Method.

It was found that aluminum is a ductile material in which the cracks generate dislocations, blunting the cracks. The blunting and the dislocation shielding reduce the local stress intensity factor. Also, twinning, which has not been observed experimentally in Aluminum due to the high stacking fault, was obtained in the simulation. Probably, the low temperature facilitates twin formation.

The applied stress intensity factor required to propagate the crack tip increases at first, and then becomes constant as the maximum distance that the first dislocation can travel away from the crack tip increases. These effects can be attributed to dislocation shielding and crack blunting. The maximum distance of the emitted dislocations from the crack tip is the equilibrium distance for the largest simulation performed (400,000 atoms) while for the smaller simulations the dislocations are hindered by the fixed boundary condition of the model. On the other hand, the total local stress intensity factor at the crack tip and the local stress intensity factor along the slip plane remain basically

constant as the maximum distance of the emitted dislocations from the crack tip increases. For distances larger than  $300A^0$ , these local stress intensity factors start to increase slightly.

# Acknowledgements

I would like to thank Dr. Diana Farkas, my advisor, for letting me join her group. It was a pleasure to work under her guidance and supervision. Her patience, advice and constructive comments taught me much, and I am truly indebted to her.

Dr. William Curtin was of great contribution for this work. His help, comments and kindness were greatly appreciated.

Also I would like to thank Dr. William Reynolds and Dr. Herve Marand for making time in their busy schedules to serve on my committee.

Special thanks to Dr. Yuri Mishin for his limitless patience, help about his code, and invaluable discussion.

To Dr. Semih Olcmen, many thanks for reading my manuscript and his helpful comments.

I would like to thank my wife, the most wonderful woman, for her support and patience.

This work was sponsored by the Office of Naval Research and National Science Foundation.

# Contents

|   |            |
|---|------------|
| <b>Acknowledgments</b>  | <b>iv</b>  |
| <b>List of Figures</b>  | <b>vii</b> |
| <b>1 INTRODUCTION AND BACKGROUND</b>                                | <b>1</b>   |
| 1.1 Introduction.....   | 1          |
| 1.2 Nature of the Plastic Deformation.....                          | 4          |
| 1.3 Dislocations.....   | 5          |
| 1.4 Perfect and Imperfect Dislocations .....                        | 6          |
| 1.5 Stacking Faults and Partial Dislocations in FCC Crystal .....   | 7          |
| 1.6 Mechanical Twinning in FCC Crystals .....                       | 8          |
| 1.7 Slip Planes in the FCC Structure .....                          | 10         |
| 1.8 Fracture Modes and Dislocation Emission from the Crack Tip..... | 10         |
| 1.9 The Effects of Emitted Dislocations on the Crack Tip .....      | 11         |
| 1.10 The Griffith Relation .....                                    | 11         |
| 1.11 Ductile versus Brittle Behavior.....                           | 12         |
| 1.12 The Emission Criterion .....                                   | 15         |
| 1.13 Lattice Resistance .....                                       | 17         |
| <b>2 THE THEORY OF DISLOCATION CRACK INTERACTION</b>                | <b>27</b>  |
| 2.1 Introduction.....   | 27         |
| 2.2 Force on a Dislocation.....                                     | 28         |
| 2.3 Dislocation Emission .....                                      | 29         |
| 2.4 Dislocation Shielding.....                                      | 31         |
| 2.5 Model .....   | 32         |

|          |   |           |
|----------|---|-----------|
| 2.6      | Shielding by External Dislocation ..... | 34        |
| <b>3</b> | <b>ATOMISTIC SIMULATION OF FRACTURE</b> | <b>40</b> |
| 3.1      | Introduction.....                       | 40        |
| 3.2      | The Embedded-Atom Method.....           | 41        |
| 3.3      | Interatomic Potential .....             | 42        |
| 3.4      | Simulation Technique .....              | 43        |
| <b>4</b> | <b>SIMULATION RESULTS</b>               | <b>46</b> |
| 4.1      | Introduction . .....                    | 46        |
| 4.2      | Twin formation.....                     | 49        |
| 4.3      | Geometry of the Crack Tip.....          | 50        |
| 4.4      | Shielding.....                          | 52        |
| 4.5      | Pinning Distance .....                  | 54        |
| <b>5</b> | <b>DISCUSSION</b>                       | <b>70</b> |
| <b>6</b> | <b>CONCLUSIONS</b>                      | <b>73</b> |
|          | <b>References</b>                       | <b>75</b> |
|          | <b>Notation</b>                         | <b>78</b> |
|          | <b>Vita</b>                             | <b>79</b> |

# List of Figures

|            |  |    |
|------------|--|----|
| Figure 1.1 | Shear displacements.....   | 18 |
| Figure 1.2 | Atomic displacement associated with twinning .....   | 19 |
| Figure 1.3 | Illustration of the two dislocations.....  | 20 |
| Figure 1.4 | Three types of stacking positions in an FCC crystal.....   | 21 |
| Figure 1.5 | Twinning in an FCC crystal.....  | 22 |
| Figure 1.6 | A twin orientation is produced in an FCC crystal .....   | 23 |
| Figure 1.7 | Three modes of fracture and crack tip deformation.....   | 24 |
| Figure 1.8 | A plate containing elliptical cavity subjected to a uniform applied stress..   | 25 |
| Figure 1.9 | Crack tip slip plane geometry for dislocation emission from a mode I crack.....  | 26 |
| Figure 2.1 | Coordinate system for a crack and an emitted dislocation .....   | 36 |
| Figure 2.2 | Force on a dislocation in the vicinity of a crack .....  | 37 |
| Figure 2.3 | Emission surface in k-space .....  | 38 |
| Figure 2.4 | Angular plot for stress intensity factors.....   | 39 |
| Figure 3.1 | A computational block .....  | 45 |
| Figure 4.1 | Some steps of two different simulation blocks.....   | 57 |
| Figure 4.2 | The total local stress intensity factor versus the applied stress intensity factor .....   | 64 |
| Figure 4.3 | Some steps after the first dislocation is stopped by the fixed boundary ....   | 65 |
| Figure 4.4 | The applied stress intensity factor, the local stress intensity factor at the crack tip, and the local stress intensity factor along the slip plane versus the maximum distances of the emitted dislocations ..... | 67 |
| Figure 4.5 | The applied stress intensity factor, the total local stress intensity factor at the crack tip, and the local stress intensity factor along the slip plane versus the number of emitted dislocations .....          | 68 |
| Figure 4.6 | The effect of the maximum distances on the number of dislocations emitted.....   | 69 |

# Chapter 1

## Introduction and Background

### 1.1 Introduction

Cracks and dislocations are related lattice defects, which jointly provide an answer to understanding the failure mechanisms in crystalline materials. A fully ductile material like high purity copper fails by continuous necking when it is stressed above its elastic limit. The necking failure in this crystalline case involves only dislocation processes, and it is termed *plastic rupture*. A fully brittle material such as glass or mica fails when a single crack traverses the material, leaving it in two parts.

Nearly all crystalline materials fail by a combination of these two processes: namely, cracks and dislocations interact strongly with each other often in very complex ways. Toughness is an important concept to describe the dislocation interactions with the cracks, and from this to establish the fracture criterion, because a desirable structural material is one which has both high strength and high toughness. The toughness may be defined as the energy absorbed per unit length of advance of a crack.

Qualitatively, crystalline materials are strong due to the interaction of dislocations with themselves, with cracks, and with other imperfections. Perhaps the greatest difficulty is underlying mechanisms of these interactions.

Although a failure may appear macroscopically to be crack-like, on closer microscopic examination the crack will be found to be quite blunt and irregular in shape, without the characteristic atomically-sharp tip of the cleavage crack. On the other hand, a crack showing considerable toughness may consist of a sharp underlying crack, but be associated with a large number of dislocations. Moving from relatively ductile to relatively brittle materials, the shape of the crack changes from a blunt notch or rounded hole which expands by purely plastic means (i.e., dislocation formation from material ahead of the crack or from the corners of the crack surface) to a crack which advances by cleavage.

The toughness problem can be approached by distinguishing between an intrinsically brittle material and an intrinsically ductile one in terms of crack propagation and a material relaxation mechanism. Ductile fracture is associated with ease of dislocation nucleation, as well as ease of dislocation motion on slip planes which can be a precursor for crack propagation through void growth ahead of the crack tip. On the other hand, brittle fracture is associated with very little dislocation mobility or atomically-sharp crack, which is unstable in the lattice without breakdown by dislocation nucleation. This distinction between an intrinsically brittle or ductile crack may depend on external conditions and the material itself.

Understanding why a given material stands where it does on the ductile brittle axis is a primary goal of materials science, and this is equivalent, of course, to understanding quantitatively the fracture toughness of materials. Unfortunately, the goal has not been realized yet.

To understand crack tip behaviors, two types of models have been developed: continuum and atomistic. As an example of the continuum, the Rice and Thomson model [1] proposed a condition for dislocation emission from a crack tip based on elastic interaction between a crack and a dislocation. The model used the Griffith relation (discussed in Section 1.10) for cleavage requirements. Also the model showed that the ratio  $g/m\mathbf{b}$  was a good indicator of the ductile versus brittle behavior of a material,

where  $\gamma$  is surface energy,  $\mu$  is shear modulus and  $b$  is Burgers vector. The Atomistic model was studied by Xu *et al.* [2]. They made some improvements to the previous method. However, the model can not be used to study initially-blunted cracks because of the assumption that crack tips are atomically sharp, and remain so during the dislocation nucleation event.

A blunted-crack configuration has generated some interest-limited attempts at evaluating its effect and determining why its stress field is different from the sharp crack stress field. Especially, the role of the crack blunting by external dislocations on dislocation emission and on a crack behavior has been studied hardly at all. These put quantitative study of the structure of cracks still largely in the *research to be done category*. In this study, therefore, we will study effects of dislocation emission from a mode I crack tip, and of pinning distances on the crack behavior and fracture toughness.

In this study, the well-known dislocation emission model, the Rice and Thomson model [1], which gives a quantitative criterion for ductile versus brittle behavior, is compared with atomistic. The model has fair success in predicting the local stress intensity factor contributed by an emitted dislocation along an inclined slip plane and has been largely successful in explaining the intrinsic cleavability of crystals, i.e. in dividing crystals into those that never cleave (most FCC metals, alkali metals) and those that cleave at low temperature (covalent crystals, most BCC transition metals).

All calculations in the study are performed for cracks in a face-centered cubic (FCC) metal, aluminum (Al). The first reason for this choice is that aluminum is one of the most commonly used metals, and thus its behavior under load is well known and can be easily compared with the behavior in simulation. The second reason is the availability of simple, yet reliable interatomic potentials, namely the Embedded Atom Method (EAM) [3,4] potentials for aluminum.

## 1.2 Nature of the Plastic Deformation

Plastic deformation is inhomogeneous because it occurs by the shearing of whole blocks of crystal over one another (Figure 1.1) rather than by continuous and homogeneous deformation where atoms are displaced the same amount from their equilibrium lattice positions as in elastic deformation (Figure 1.1). The shear displacements occur by either the process of slip (glide) or twinning. Slip always occurs by displacement of blocks of the crystal in specific crystallographic directions called *slip directions*. It usually takes place on particular lattice planes called *slip or glide planes*.

Plastic deformation in crystals can also occur by twinning, where layers of atoms slide in such a manner as to bring the deformed part of the crystal into a mirror image orientation relative to the undeformed part of the crystal. As shown in Figure 1.2, the plane AB across which twinning occurs is called the *twinning plane* and twinning, like a slip, occurs in a specific direction called the *twinning direction*.

In a single crystal, macroscopic plastic deformation (yielding) occurs when the applied tensile stress  $\mathbf{s}$ , resolved as a shear stress  $\mathbf{t}$  on a particular slip plane and in a particular slip direction, is equal to a critical value ( $\mathbf{t} = \mathbf{t}_y = k$ ). The yield criterion is therefore

$$\mathbf{s} \cos \mathbf{q} \cos \mathbf{f} = \mathbf{t}_y = k \quad (1.1)$$

where  $\mathbf{f}$  is the angle between the tensile axis and the slip or twin direction,  $\mathbf{q}$  is the angle between the normal of the slip or twin plane and tensile axis, and  $k$  is the yield stress in pure shear (torsion loading).

The particular mode of deformation is determined by the criteria that are satisfied at the lowest value of  $\mathbf{t}_y$ . The yield stresses for slip or twinning are not a constant for a given material but vary with test temperature, strain rate, grain size, and other extrinsic and intrinsic variables. In most materials having body centered cubic structure, generally the yield stress for slip increases sharply with decreasing temperature, whereas the twinning stress is relatively independent of temperature. At most temperatures,  $\mathbf{t}_y$

$(\text{slip}) < \tau_y(\text{twin})$  and slip is the preferred mode of the deformation, but at very low temperatures, the stress necessary for twinning is less than that required for slip, and twinning is the preferred mode of the deformation. In FCC metals, such as copper and aluminum, the twinning stress is so much higher than the stress required for slip that twinning is generally not observed [3-5].

### 1.3 Dislocations

Slip is the sliding of blocks of the crystal over one another along definite crystallographic planes. This process is made possible by presence of numerous linear defects in the lattice called *dislocations*. The local area in the lattice between the slipped and the unslipped region is what is called the *dislocation*. Crystals, thus, flow plastically by the motion of dislocations on the application of a small force. Fatigue, creep, brittle fracture, and yield point are important for explaining the slip of a crystal as well as the dislocations. Two parameters are necessary to classify a dislocation: Burgers vector and the dislocation line direction. The Burgers vector presents the amount of displacement between the slipped and the unslipped regions and is determined by drawing a circuit around the dislocation in the unslipped part of the lattice. The line direction is defined by the unit vector tangent to the dislocation line.

There are three kinds of dislocations: *edge*, *screw* and *mixed*. The edge dislocations correspond to an extra half-plane inserted between two crystallographic planes in the lattice (Figure 1.3) A defining characteristic of such a dislocation is that its Burgers vector is always perpendicular to the dislocation line. A screw dislocation (Figure 1.3) can be constructed by cutting a pathway through a perfect crystal, then skewing the crystal one atom spacing. The Burgers vector is then parallel to the dislocation line. Aside from the extreme cases where the Burger vectors is either normal to the dislocation axis (edge dislocation) or parallel to it (screw dislocation), any intermediate orientation is possible. Such intermediate dislocations are referred to as *mixed*. Mixed dislocations may be regarded, in all respects, as the superimpositions of an

edge dislocation (the so-called *edge-component*) and a screw dislocation (named the *screw-component*).

## 1.4 Perfect and Imperfect (Partial) Dislocations

A dislocation in a particular crystal is completely described by its Burgers vector and its axis. Burgers vector is determined partly by the crystal structure and partly by energy considerations.

The geometry of the crystal structure fixes the position in which atoms may be translated so as either to maintain a perfect lattice (an identity translation) or to develop a new configuration such as a twinned structure, which is mechanically stable. The characteristic Burgers vectors of crystal dislocation must give one or the other of these two kinds of translations, since a mechanical unstable configuration cannot exist. Dislocations fall into two categories: perfect or imperfect (partial). Perfect dislocations' Burgers vector produce identity translation while Burgers vectors of partial (imperfect) dislocations cause atoms to lie in a different position after they move through the lattice.

An important case is that for which  $\mathbf{b}$  is a lattice vector and  $b$  is one lattice spacing, since this is the smallest amount of slip which leads to a final configuration in the crystal identical to the initial one. A dislocation with this vector is called a *unit dislocation*. As an example, in the simple cubic lattice of spacing  $a$ , the unit vectors are  $a[100]$ ,  $a/\sqrt{2}[110]$  and  $a/\sqrt{3}[111]$ .

Because the energy of a dislocation is proportional to  $b^2$ , it is possible for some unit dislocations to decompose into two partial dislocations that have a lower energy than their parent has. The two partial dislocations will try to repel each other, when their Burgers vectors have a parallel component. However, the atoms between two partials are not in their normal positions and a stacking fault is formed. The separation distance between the two partials is governed by the energy of the fault. When the stacking fault energy is low, the partials are widely extended; in materials with high stacking fault energy the partials are close together.

## 1.5 Stacking Faults and Partial Dislocations in FCC Crystals

For closed packed FCC, the interatomic forces are such that it is a fair approximation to regard the atoms as a hard spherical ball held together by attractive forces. These structures are generated by stacking closed packed layers on top of one another in the fashion shown in Figure 1.4. Given a layer  $A$ , closed packing can be extended by stacking the next layer so that its atoms occupy  $B$  or  $C$ . Here  $A$ ,  $B$ , and  $C$  refer to the three possible layer position in a projection normal to the closed packed layer. A closed packed structure is generated, provided that no two layer of the same letter index, such as  $AA$ , are stacked in juxtaposition to one another. The sequence corresponding to an FCC crystal is  $\dots ABCABC\dots$  or  $\dots CBACBA\dots$ . In FCC crystals one distinguishes two basic types (Frank [8]), one of them is equivalent to the removal of the atomic plane,  $\dots ABCBCA\dots$ , named the *intrinsic stacking fault*, and the other is equivalent to the intersection of an extra plane,  $\dots ABCACBA\dots$ , the *extrinsic fault*.

The shortest lattice vector in FCC is  $a/2[110]$ , which joins an atom at a cube corner to a neighbor at a faced center, and defines the observed slip direction. The other unit vector in the cubic cell,  $a[100]$ , can dissociate into  $a/2[110] + a/2[\bar{1}\bar{1}0]$ , but there is no gain of elastic energy when this happens.

Unit dislocations, which lie in closed-packed planes, can lower their energies by dissociating into imperfect dislocations, so called *half dislocations* of Heidenreich and Shockley [7]. Partial dislocations are important in the twinning reaction, in phase transformation, and in the formation of dislocation barriers by intersecting dislocations. The extension of the perfect dislocation into partials bounding a stacking fault affects the climb and cross slip of dislocations. Stacking faults themselves are important barriers to dislocation motions.

To understand how the unit dislocations dissociate into imperfect dislocations, consider first the process of slip plane in Figure 1.4. The Burgers vector  $\mathbf{b}_1 (= a/2[10\bar{1}])$  defines one of the observed slip directions. On the other hand, as Thompson and

Millington [10] have pointed out, if atoms are regarded as balls rolling over the plane, then the one in position of the type  $B$  on the plane would move most easily towards a neighboring position of the type  $C$ . This is because of the motion of the atom along the straight path from  $B \rightarrow B$  involves larger dilatation normal to the slip plane, and hence a larger misfit energy than does motion along the path  $B \rightarrow C \rightarrow B$ . It is expected that, when a slip movement takes place macroscopically along  $[10\bar{1}]$ , the atoms move in a zigzag path of the type  $B \rightarrow C \rightarrow B$  following the vectors  $\mathbf{b}_2 (=a/6[2\bar{1}1])$  and  $\mathbf{b}_3 (=a/6[1\bar{1}2])$  alternatively. If the slip takes place from the  $B$  to  $C$  position the order of stacking of (111) layers in the crystal is changed. In an FCC lattice, these planes are stacked on one another in a sequence of the type ...  $ABCABCABC...$ , so that slip along a vector such as  $\mathbf{b}_2$  between two of these planes produces a fault such as .. $ABCACABC...$  in the sequence. This stacking fault causes a thin layer of the material to have a close-packed hexagonal structure ...  $CACA...$  It does not affect the two types of packing of the nearest neighbors in the crystal and so should not increase the energy.

The intrinsic stacking fault and its associated shear can be produced by the motion of the partial dislocation. The fault is removed, restoring the perfect lattice arrangement behind the dislocation, by the subsequent glide of the partial. Partial dislocations of the type  $1/6\langle 112 \rangle$ , which are glissile on the  $\{111\}$  planes, are called *Shockley partial* [9]. Figure 1.4 shows the dislocation of a perfect dislocation into an extended dislocation consisting of two Shockley partials and an enclosed stacking fault.

## 1.6 Mechanical Twinning in FCC Crystals

The deformation of a crystal occurs by the passage of the perfect dislocations across a slip plane. The movement of a single perfect dislocation across a slip plane shears the crystal by an atomic distance. Although atoms move with respect to each other across the slip plane, they move into a crystallographically equivalent position.

When the partial dislocations move across various slip planes during the deformation, the atoms on either side of the slip planes are not moved into equivalent positions. If one partial dislocation were to move across each individual slip plane of a set of parallel slip planes, the orientation of the crystal actually would be changed. Figure 1.5 shows that how the stacking sequence of the closed packed plane in FCC lattices changed if the partial dislocations shown in the left-hand side of Figure 1.5 (a) move across the planes and end up at the right-hand side of Figure 1.5 (b). The stacking sequence  $ABCABCABC$  is changed to  $ABCA\uparrow CBACB$ , where the dagger denotes a fault in the stacking sequences.

The two crystals, which form the bi-crystal of Figure (b) are said to be in a twin orientation with respect to each other. A bicrystal with the same relative orientation between its component crystals can be formed from sections of the two identical FCC single crystals shown in Figure 1.6. To make a twinned crystal, the plane EFG and E'F'G' are joined by superimposing E and E', F and F', and G and G'. The extra plane of atoms at the boundary then is removed. The crystal mirror image of one other can be seen

Mechanical twins are made in FCC crystals by a slip across  $\{111\}$  planes. The amount of slip across each plane is not equal to an atomistic distance. If a Shockley partial dislocation  $(a/6)\langle 112 \rangle$  traverses each  $\{111\}$  plane the sequence

||  
 $ABCABCABCABC$

is transformed to  $ABCABACBAC$

FCC matrix || twin.

A mirror image of the stacking sequences of the  $\{111\}$  planes has been produced relative to the unshered plane (B). This mirror symmetry is a characteristic of the twinning.

## 1.7 Slip Planes in the FCC Structures

Slip is anisotropic; it occurs more readily along certain crystal planes and directions than along others. Many investigations have established that the slip direction is almost always along the atoms that are most closely packed. The results of the studies indicate that  $\{111\}\langle 110\rangle$  is the major operative slip system in the FCC structure. The  $\{111\}$  planes are the most densely packed planes in FCC metals, and also the planes on which stacking faults form.

There are two unusual slip systems: the first is  $\{100\}[110]$  slip at elevated temperatures. The second slip  $\{110\}[110]$  has been observed optically at high temperatures.

## 1.8 Fracture Modes and Dislocation Emission from the Crack Tip

Real cracks are three-dimensional defects whose fracture planes may be rough surfaces. Even brittle fractures may take place on the three dimensional network of a grain boundary structure, and that interaction with various kinds of imperfections in a material is common. Nevertheless, for analytical purposes, it is desirable to idealize a crack line as a one-dimensional line defect on a flat cleavage plane. There are three modes of cracks corresponding to the different orientations of external stress with respect to the fracture plane. These three modes are analogous to the two different classes of dislocations: screw and edge. In the case of the crack, a cut is made in the medium, which becomes the cleavage plane, and simple shear or tensile stress is exerted on the external surface of the specimen. In mode I (opening mode), the stress is a tensile stress with principle axis normal to the cleavage plane, and under mode I loading edge dislocations are emitted on one inclined slip plane simultaneously as shown in Figure 1.7. The Burgers vectors of these dislocations are in the direction parallel to the tensile stress. The displacement generated by this crack deformation is parallel to the crack-opening displacement (COD). In mode II (sliding mode), the stress is a shear stress, which is in the plane of the crack normal to the crack line, and under mode II loading,

edge dislocations are emitted only on one of the inclined slip planes. The displacement generated by mode II crack deformation is parallel to the direction of the dislocation motion. In mode III (tearing mode), the stress is a shear stress, which is in a plane along the crack line. Under mode III loading, screw dislocations are emitted, which on the slanted slip plane give rise to mode III crack deformation, and the displacement is parallel to the crack front (Figure 1.7).

## 1.9 The Effects of Emitted Dislocations on the Crack Tip

Crack tip generated dislocations produce two effects. First, they reduce the applied stress intensity factor at the crack tip by shielding [1,11,12]. The dislocation crack tip shield is a negative stress intensity factor that reduces the applied stress intensity factor at the crack tip. Secondly, crack tip dislocation emission changes the geometry of the crack tip; edge dislocations with a component of the Burgers vector normal to fracture plane blunt the crack tip [1,13]. Screw dislocations with a Burgers vector component normal to the fracture plane jog the crack plane [13-16]. Thus the crack tip dislocation generation helps reduce some crack tip stresses and changes the crack tip geometry and bonding.

## 1.10 The Griffith Relation

In this section, we will review the classic work of Griffith on the equilibrium of cracks in brittle materials [17]. The Griffith relation is a simple equation of balance between elastic driving force on the crack and the lattice resistance associated with the energy of the growing surface.

It will be assumed that the crack of Figure 1.8 is loaded in mode I. Then, since there is no dislocation present, the elastic force per unit length on the crack is given by

$$f_c = \frac{(1-\mathbf{n})}{2\mathbf{m}} k_I^2 \quad (1.2)$$

where  $\mathbf{m}$  is shear modulus,  $\mathbf{n}$  is Poisson's ratio, and  $k$  refers the stress intensity factor for mode I tensile deformation. This force is called the *energy release rate* in the

mechanics literature. Opposing this elastic force is a resistive force to crack opening provided by the material. Working by a simple analog to soap bubble-like surface tension in a solid, the opposing force per unit length exerted on the crack by a crystal is simply given by

$$f_{crystal} = -2\mathbf{g} \quad (1.3)$$

where  $\mathbf{g}$  refers to the true surface energy of the crack plane. It should be noted that there are two surfaces presented to the crack tip.

When the elastic forces and surface tension forces are in balance, then the point of equilibrium is given by the critical value of  $k$  where

$$k_{Ic} = 2\sqrt{\mathbf{gm}/(1-n)} \quad (1.4)$$

This equation is often called the Griffith relation, although it is not in the form given by him, since the stress intensity factor was introduced much later.

## 1.11 Ductile versus Brittle Behavior

In the fundamental paper for differentiating ductile versus brittle behavior, Kelly, Tyson and Cottrell [18] have pointed out that solids can be classified as *inherently brittle* if, at the crack tip of an atomically sharp crack in the stressed solid, the ideal cohesive strength is reached before the ideal shear strength. Based on simple and straightforward considerations, they were able to conclude that some covalent solids, such as diamond and alumina, should be inherently brittle, while the closed packed set of face-centered cubic metals, such as copper, silver and gold, should be inherently ductile. In most other cases, the simple criterion of Kelly *et al.* has proven to be too crude for quantitative predictions. Rice and Thomson [1] have removed some of the weak features of the model of Kelly *et al.* by considering in detail the critical configurations for nucleation of the dislocation loops in the highly inhomogeneous stress field of the crack tip. This has permitted a more precise statement of the borderline condition between inherent ductility and inherent brittleness, but has still provided to be indecisive for many technologically important materials.

According to Rice and Thomson, in the region very close to the crack tip, the shear stress varies very rapidly, and ideal shear strength should not be used. They argued that the blunting of the crack tip requires the production or annihilation of dislocations of Burgers vector with a component normal to the crack plane. They calculated the forces acting on the dislocation in the vicinity of the crack tip and found that if  $\frac{mb}{g} > 7.5-10$ , there will be an activation energy barrier to the formation of dislocations. The material therefore will be classified as *brittle*. If  $\frac{mb}{g} < 7.5-10$  dislocation will be emitted and will move away from the crack, blunting the crack by one atom spacing and the material will be classified as *ductile*. A model inspired by Rice and Thomson [1] was proposed by Ohr and Chang [19]. They describe the plastic zone at the crack tip by linear pileup dislocations. They define a critical value,  $k_g$ , for the stress intensity factor above of which there will be spontaneous generation of dislocations. If  $k_g < k_c$ , dislocations are nucleated and move away from the crack tip. Also these dislocations pile up to form the plastic zone.

These theories imply that dislocation emission prevents the crack from propagating. However, the emission of the dislocation at the crack tip does not always imply a ductile behavior, and there are experimental evidence that dislocation emission can occur during the crack propagation [20-22]. Bond breaking and dislocation emission, therefore, can be concomitant phenomena at the crack tip. Lin and Thomson [23] showed that combined cleavage and dislocation emissions were possible under the specific conditions of loading. In their extensive overview of cleavage, dislocation emission and shielding for cracks under general loading, Lin and Thomson [23] developed a simple crack stability diagram in a three-dimensional local k-space. They found that the emission of dislocations depended on the particular slip system involved, as well as the loading configuration. From the crack stability diagram, whether cleavage, dislocation emission or a combination of both will take place can be predicted under any mixed loading. Two important conclusions can be deduced from their analysis. Firstly,

only dislocations generated by mode I (pure tensile loading) can blunt the crack. Secondly, the cleavage criterion depends only on the local mode I stress intensity factor  $k_I$ . They, however, do not take into account the fact that branching of the crack to a new cleavage system could occur.

Rice has presented the most recent theory on the competition between crack propagation and dislocation nucleation [24]. In this theory, a periodic relation between shear stress and atomic shear displacement is assumed after the Peierls concept [25]. When a small load is applied at the crack tip, a small amount of slip takes place, which can lead to a fully-formed dislocation. The resistance to dislocation nucleation is taken as being proportional to the unstable stacking energy  $g_{us}$ . In a block like sliding of one half the lattice relative to the other half along a slip plane,  $g_{us}$  is the maximum energy encountered. The crack will be blunted by dislocation emission if the resistance to dislocation nucleation is overcome before the resistance to cleavage. Rice calculated the condition of the dislocation emission before crack extension as

$$\frac{g_s}{g_{us}} > b$$

where the value of  $b$  depends on the anisotropy and the angle between the slip plane and the loading direction or the cleavage plane and the loading direction. The Rice theory predicts for instance that aluminum is ductile under pure mode I loading.

Finally, Zhou *et al.* [26] used lattice static simulations in two-dimensional hexagonal crystal to show that ledge effects alter the crossover condition. They obtained the crossover condition

$$\frac{g_{us}}{mb} = b'$$

which is independent of  $g_s$  and where  $b'$  depends on the anisotropy and the angle between the slip plane and the loading direction or the cleavage plane and the loading direction.

## 1.12 The Emission Criterion

Recently, Rice [24] has shown that a Griffith-like relation can also describe the emission dislocation criterion for a crack in pure mode II loading, in which the dislocation is emitted directly in front of the crack in a non-blunting configuration. The emission criterion is believed to be a part of the criterion for intrinsic ductility of the material, because if the lattice fails in dislocation emission before it fails in cleavage, then the material is ductile and vice versa.

Rice identified a solid state parameter, the unstable stacking energy  $\mathbf{g}_{us}$ , which characterizes the resistance to displacement along the slip plane, and thus to dislocation nucleation. It is the maximum energy barrier encountered in block-like sliding along the slip plane, of one half of the crystal relative to the other. Thus, it provides the simplest measures of the effects of the discreteness of the crystal structure. In terms of  $\mathbf{g}_{us}$ , the emission criterion is given by

$$k_{Ie}(\mathbf{q} = 0) = \sqrt{2\mathbf{g}_{us} \mathbf{m}/(1-\mathbf{n})} \quad (1.5)$$

where  $\mathbf{q}$  is the inclination of the slip plane. This approach has advantages, such as  $\mathbf{g}_{us}$  can be accurately calculated by several existing first-principle total energy methods.

When a dislocation is emitted at a non-zero angle to the crack plane, the crack is blunted and should be more difficult to cleavage. Therefore, the true intrinsic ductility criterion should be related to such a blunting emission configuration. In the non-zero angle case,  $\mathbf{q} \neq 0^0$ , neglecting the ledge effect caused by dislocation emission, the emission criterion in mode I crack is given by

$$k_{Ie} = \left[ \frac{2\mathbf{m}\mathbf{g}_{us}}{1-\mathbf{n}} \frac{8}{(1+\cos\mathbf{q})\sin^2\mathbf{q}\cos^2\mathbf{f}} \right]^{1/2} \quad (1.6)$$

Where  $k_I$  refers to the mode I crack tip stress intensity factor and  $\mathbf{q}$  is the inclination of the slip plane.  $\mathbf{f}$  is the component of the angle mode by Burgers vector with the dislocation line as shown in Figure 1.9.

In the case of  $\mathbf{f} = 0^0$ , Equation 1.6 becomes,

$$k_{Ie} = \left[ \frac{2\mathbf{m}\mathbf{g}_{us}}{1-\mathbf{n}} \frac{8}{(1+\cos\mathbf{q})\sin^2\mathbf{q}} \right]^{1/2}. \quad (1.7)$$

A crossover in a crack tip behavior may occur, for example if  $\mathbf{g}_{us}$  becomes so large that cleavage directly ahead of the crack requires a lower  $k_I$ . The transition from one mode of instability to another occurs when  $k_{Ie} = k_{Ic}$ , using values of  $k_{Ie}$  and  $k_{Ic}$  from Equations 1.7 and 1.4 respectively. Rice [24] identifies a crossover condition to distinguish between shear instability on an inclined plane at angle  $\mathbf{q}$  and cleavage on the plane directly ahead of the crack:

$$q \equiv \frac{\mathbf{g}_{us}}{2\mathbf{g}_s} = \frac{(1+\cos\mathbf{q})\sin^2\mathbf{q}}{8}. \quad (1.8)$$

Therefore, the relevant material parameter is  $q$ . The dislocation will occur first if  $q$  is less than the geometric function of the slip plane angle on the right hand side of Equation 1.8.

As the dislocation is emitted in the blunting configuration, the lattice resistance is not merely due to shearing the lattice but must also involve the ledge at the crack tip of the blunted crack. Since bond breaking is usually more difficult than bond shearing, it can be expected that the ledge formation during dislocation emission may dominate the unstable stacking fault.

Zhou *et al.* [26] reformulate the emission criterion by including ledge effects. In their analysis, the critical loading to emit a dislocation on a slip plane with inclination  $\mathbf{q}$  is given by,

$$k_{Ie} \approx \left[ \frac{50\mathbf{m}\mathbf{g}_s\mathbf{g}_{us}}{b} \frac{8}{(1+\cos\mathbf{q})\sin^2\mathbf{q}\cos^2\mathbf{f}} \right]^{1/2} \quad (1.9)$$

which is not only a function of  $\mathbf{g}_{us}$  but also a function of  $\mathbf{g}$  and is independent of Poisson's ratio. Crossover condition for Zhou *et al.*'s model [26] at  $\mathbf{f} = 0^0$  is given by

$$\frac{\mathbf{g}_{us}}{\mathbf{mb}} = \left[ \frac{(1 + \cos \mathbf{q}) \sin^2 \mathbf{q}}{100(1 - \mathbf{n})} \right] \quad (1.10)$$

which is independent of  $\mathbf{g}_s$ .

### 1.13 Lattice Resistance

Lattice resistance is a resistance dislocation emission from the non-linear lattice term, such as the shear along the emission plane and the ledge effects. The total force on the emerging dislocation will be the sum of the lattice resistance and the elastic driving force, and at the critical point, these forces must be in balance to zero.

The crack will be blunted by dislocation emission if the resistance to dislocation emission is overcome before the resistance to cleavage. The resistance to dislocation emission is taken to be proportional to a new solid state parameter called the *unstable stacking energy* [34], namely

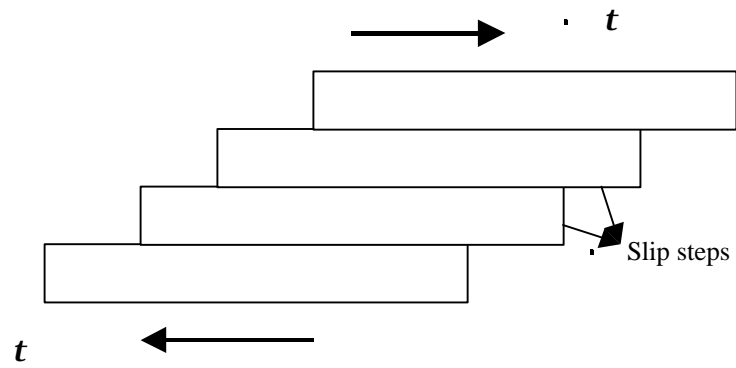
$$R_e = \mathbf{g}_{us} \quad (1.11)$$

where the unstable stacking energy is the maximum energy encountered in the block like sliding along a slip plane, in Burgers vector directions, of one half of a crystal relative to the other.

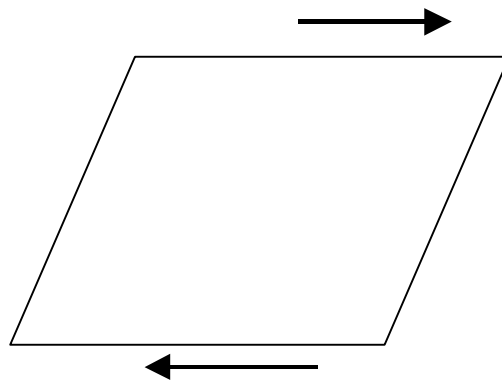
On the other hand, the lattice resistance to cleavage is as follows

$$R_c = 2\mathbf{g} \quad (1.12)$$

according to the Griffith relation.



(a) Inhomogeneous deformation.



(b) Homogenous deformation.

**Figure 1.1** Shear displacements with: (a) Inhomogeneous deformation.  
(b) Homogenous deformation.

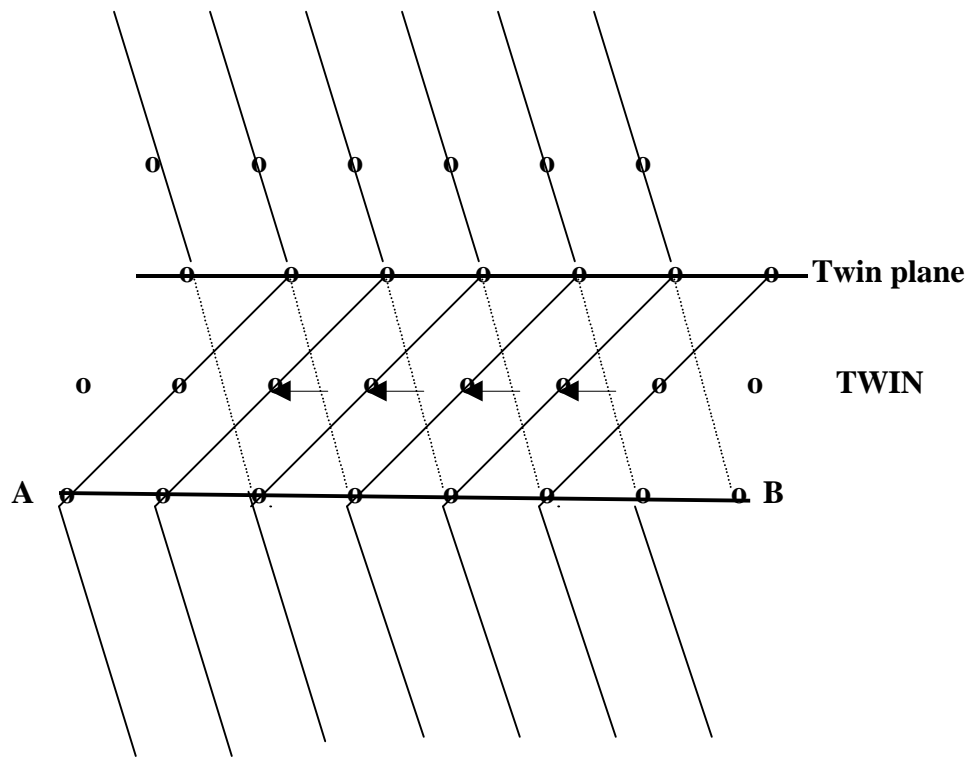


**Figure 1.2** Atomic displacement associated with twinning.

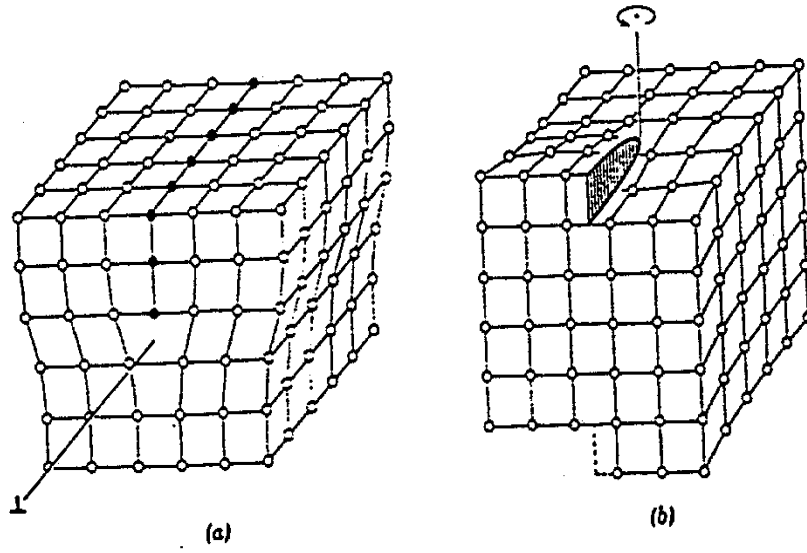
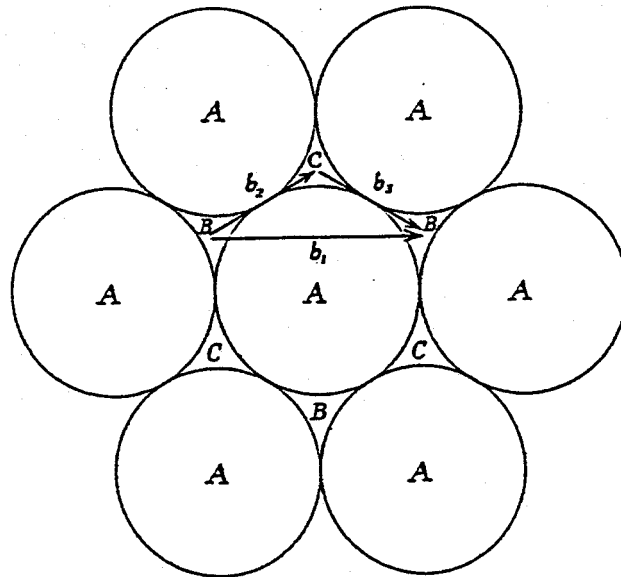


**Figure 1.3** Illustration of the two dislocations (a) an edge dislocation (b) a screw dislocation[6].



$$\mathbf{b}_1 = \frac{1}{2}[\bar{1}01]$$

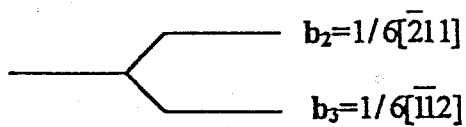


**Figure 1.4** (a) Projection normal to the (111) plane showing three types of stacking positions A, B and C. (b) Dissociation of a perfect dislocation into Shockley partials.

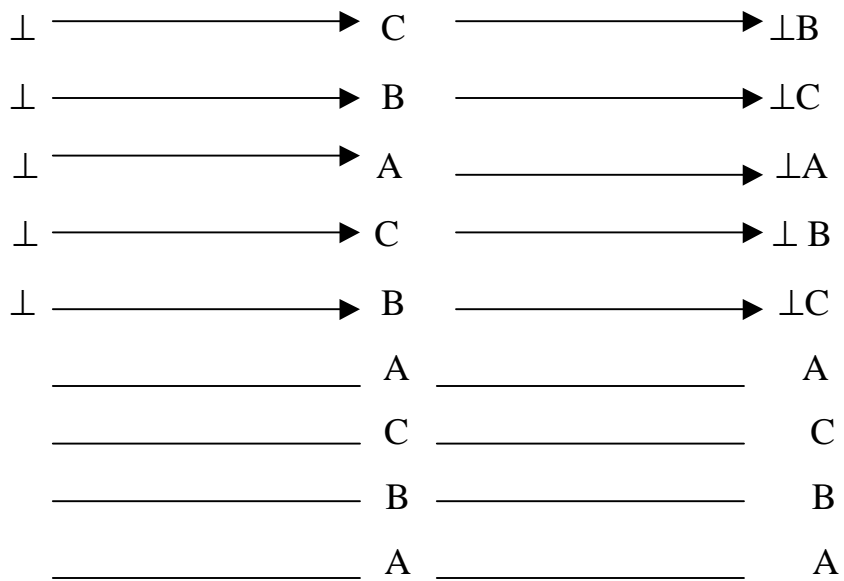


**Figure 1.5** Twinning in an FCC crystal by the passage of partial dislocations across the slip planes [6].

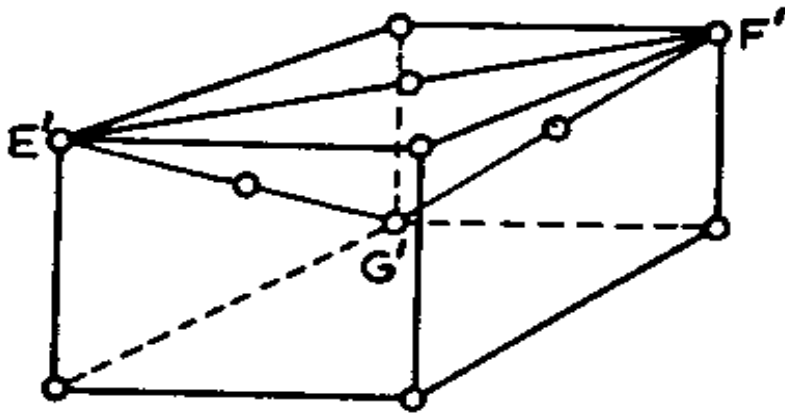
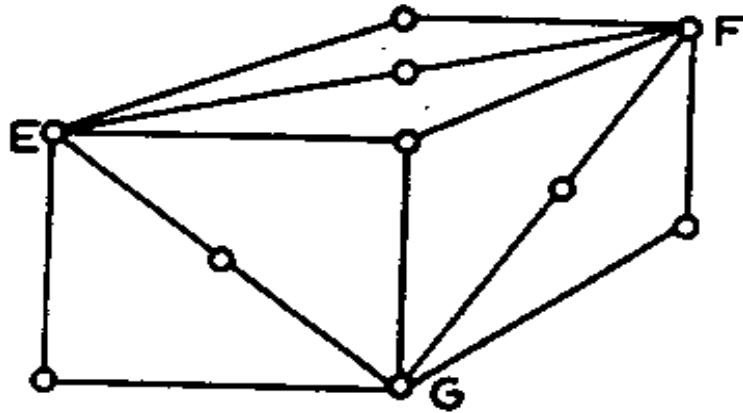


**Figure 1.6** A twin orientation is produced in an FCC crystal by joining planes EFG and E'F'G' [6].

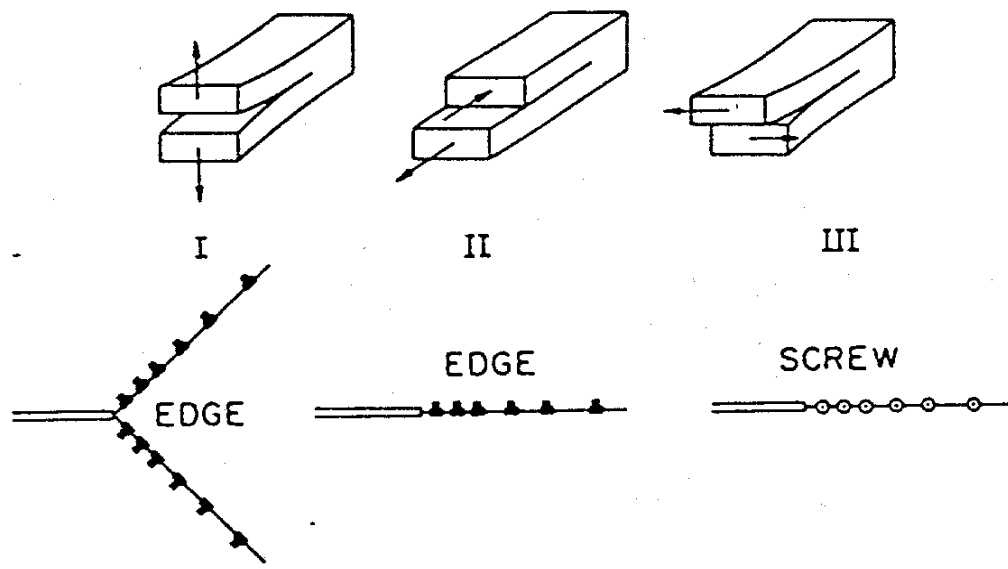


**Figure1.7** Three modes of fracture and crack tip deformation: I opening mode; II sliding mode; III tearing mode.

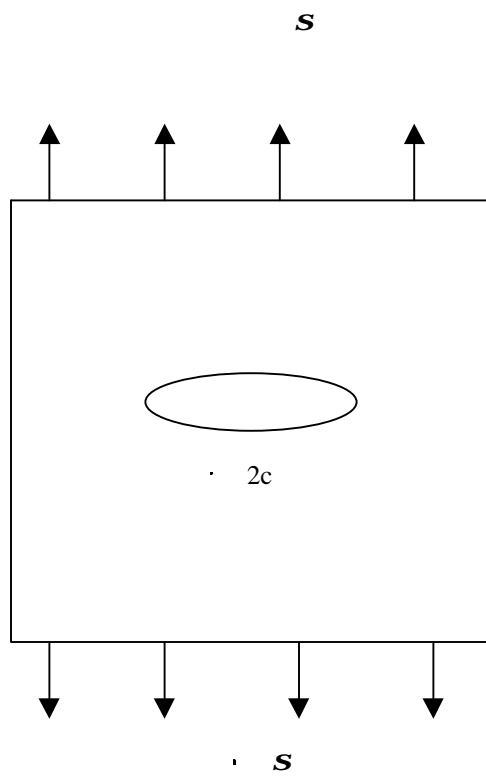


**Figure 1.8** A plate containing elliptical cavity subjected to a uniform applied stress.

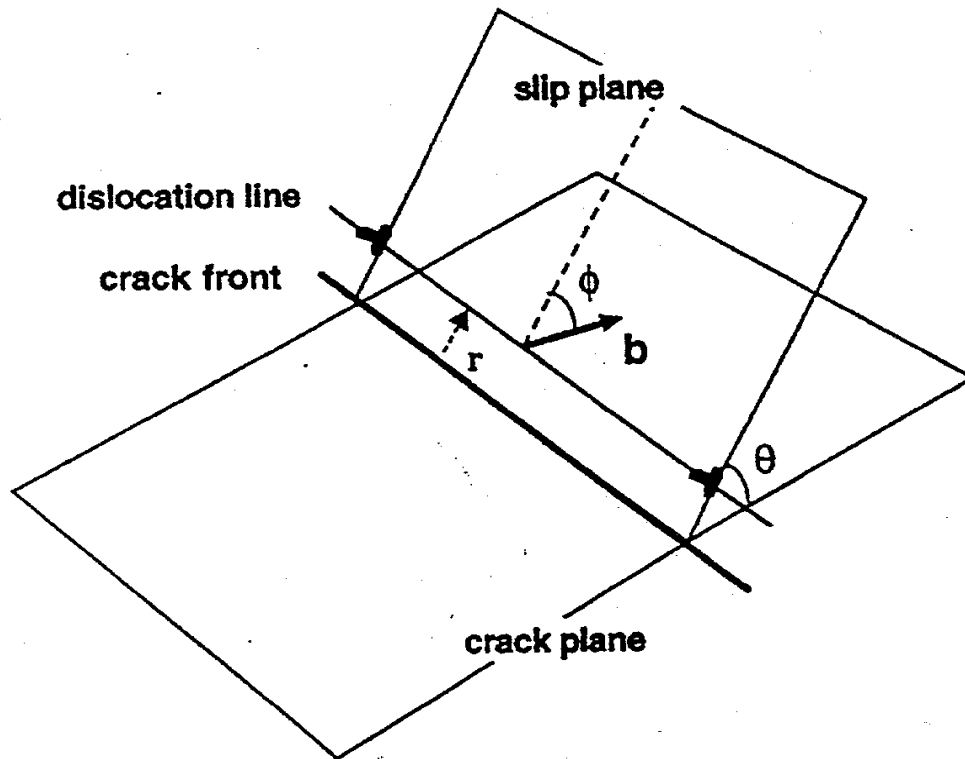


**Figure1.9** The crack tip slip plane geometry for dislocation emission from a mode I crack.

# Chapter 2

## The Theory of Dislocation-Crack Interaction

### 2.1 Introduction

In recent years, Thomson [27] has made a great deal of progress in our understanding of the dislocation-crack interaction. To observe directly the dislocation behavior at a crack tip, some experimental techniques, such as etch pits technique [28], transmission electron microscopy [29], and synchrotron X-ray topography [30], have been developed. These experiments have provided important information concerning the relationship between the crack tip stress field, the slip geometry and the distribution of dislocations near the crack tip. They also have provided direct evidence for dislocation emission from the crack tip.

Rice and Thomson [1] first treated the elastic interaction between a crack and a dislocation. They suggested a condition for dislocation emission from the crack tip based upon this interaction. Thomson [31] and Weertman [32] proposed the concept of *dislocation shielding*. The distribution of dislocation near a crack tip was studied by extending the model of Bilby, Cottrell and Swinden [33-37]. It was shown that the local stress intensity factor was lowered by shielding, and the distribution density was higher near the crack tip and decreased away from the crack tip.

## 2.2 Force on a Dislocation

Rice and Thomson [1] considered the force on a dislocation near a crack under stress. Their geometry consists of a dislocation on a slip plane that intersects the crack plane along the crack front, as shown in Figure 2.1. This dislocation is parallel to the crack front, and thus the geometry is appropriate for treating a dislocation that is emitted from the crack tip. The case of a more general geometry where the slip plane does not intersect the crack plane along the crack front was treated by Thomson [27] and Lin and Thomson [23]. According to the authors, the force on an emitted dislocation from the crack tip is composed of three terms:

$$F = F_1(Kb) + F_s(b^2) + \sum_j F_3(bb_j) \quad (2.1)$$

where  $K$  is the stress intensity factor. The first term is proportional to the product of the stress intensity factor  $K$  and the Burgers vector  $b$ . The second term is the image force. The third term refers the interaction between the emitted dislocation and other present dislocations. This is a very complicated, which was given in detail by Thomson [27] and Lin and Thomson [23]. When the slip plane intersects with the crack plane along the crack front, the expression is simplified in slip plane coordinates and becomes that of Rice and Thomson (in the absence of other dislocations). The first two terms of Equation 2.1 on the slip plane take place in the form

$$F = \frac{b_e}{\sqrt{2pr}} [K_I f_1(\mathbf{q}) + K_{II} f_2(\mathbf{q})] + \frac{K_{III} b_s}{\sqrt{2pr}} f_3(\mathbf{q}) - \frac{\mathbf{m}}{4pr} \left( \frac{b_e^2}{1-n} + b_s^2 \right) \quad (2.2)$$

$$f_1(\mathbf{q}) = \frac{1}{2} \sin \mathbf{q} \cos \frac{\mathbf{q}}{2}$$

$$f_2(\mathbf{q}) = \cos \frac{3\mathbf{q}}{2} + \frac{1}{2} \sin \mathbf{q} \sin \frac{\mathbf{q}}{2}$$

$$f_3(\mathbf{q}) = \cos \frac{\mathbf{q}}{2}$$

where  $K_I, K_{II}$  and  $K_{III}$  are components of the stress intensity factor,  $b_e$  and  $b_s$  are the edge and screw components respectively of the Burgers vector,  $\mu$  is shear modulus,  $\nu$  is Poisson's ratio, and  $r$  and  $\theta$  are the polar coordinates of the dislocation.

For an emerging dislocation, the elastic crack force from the crack tip loading, as given by the first two terms of Equation 2.2 with an inverse square root singularity, exerts a repulsive force on the dislocation, and hence will tend to drive dislocation away from the crack tip. The image force, due to image effects from the crack surfaces, the third term of Equation 2.2, is always attractive, and thus will attract the dislocation to the free surface. It is inversely proportional to  $r$ . These two forces are plotted schematically in Figure 2.2. Very close to the crack tip, the image force is greater than the crack force, and hence the dislocation is attracted to the crack tip in this region. The force on the dislocation increases with distance  $r$ , crosses the  $r$ -axis and often reaching a maximum, decreases gradually to zero at large distance. The distance at which the force on the dislocation becomes positive is inversely proportional to the square of  $K$ .

### 2.3 Dislocation Emission

As it can be seen in Figure 2.2, the force on a dislocation very close to a crack tip is attractive, so that it is difficult for a crack to emit dislocation under normal circumstances. However, the range within which a dislocation is attracted to the crack tip decreases with increasing  $K$ , i.e., with the applied stress. Rice and Thomson [1] propose that, if the applied stress is sufficiently high so that the range of attractive interaction is less than or equal to  $r_0$ , where  $r_0$  is a measure of the collective core size of a dislocation, then the emerging dislocation will always be on the repulsive side of the force distance curve. The dislocation is emitted spontaneously. In addition, Bilby *et al* [33] suggested that the force on the dislocation must be greater than the lattice frictional force,  $b\tau_f$ , in order to slip away from the crack tip.

The dislocation emission condition will be  $k > k_e$  where  $k_e$  is defined as that  $k$  for which  $F = 0$  with  $r_0$  in Equation 2.2. Thus

$$b_e [k_{Ie} f_1(\mathbf{q}) + k_{IIe} f_2(\mathbf{q})] + b_s k_{IIIe} f_3(\mathbf{q}) \geq \frac{\mathbf{m}}{\sqrt{8pr_0}} \left( b_s^2 + \frac{b_e^2}{1-\mathbf{n}} \right) \quad (2.3)$$

where  $b_e, b_s$  and  $\mathbf{q}$  are fixed by knowing the slip system, dislocation line direction and crack plane and  $r_0$  is assumed to be a material constant, approximately equal to Burgers vector of the given material. This defines a plane in  $(k_I, k_{II}, k_{III})$  space called the *emission surface* [23] as shown in Figure 2.3. The intercepts at each axis of  $(k_I, k_{II}, k_{III})$  space defined the critical stress intensity factor for emission pure loading modes and denoted by  $k_{ie}^0$  etc. as given by

$$\begin{aligned} k_{Ie}^0 &= \frac{\mathbf{m}}{\sqrt{8pr_0} f_1(\mathbf{q})} \left( \frac{b_s^2}{b_e} + \frac{b_e}{1-\mathbf{n}} \right) \\ k_{IIe}^0 &= \frac{\mathbf{m}}{\sqrt{8pr_0} f_2(\mathbf{q})} \left( \frac{b_s^2}{b_e} + \frac{b_e}{1-\mathbf{n}} \right) \\ k_{IIIe}^0 &= \frac{\mathbf{m}}{\sqrt{8pr_0} f_3(\mathbf{q})} \left( b_s + \frac{b_e^2}{b_s(1-\mathbf{n})} \right) \end{aligned} \quad (2.4)$$

$k_{ie}^0$  are functions of angle  $\mathbf{q}$ . They are shown in Figure 2.4. Spontaneous emission occurs for all values of  $k$  above the plane in Figure 2.3. However, the crack is stable against such spontaneous emission as point below the plane. It is clear that mode II loading is less than the  $k_I$  loading required for emission.

## 2.4 Dislocation Shielding

When a dislocation is emitted, there will be a repulsive force on it, and thus it is expected that the dislocation moves away from the crack tip. The force decreases as  $1/\sqrt{r}$  and the dislocation comes to rest where the crack force is in equilibrium with the lattice frictional force. The presence of the dislocation in the vicinity of the crack tip modifies the stress field of the region because of elastic interaction between the crack and the dislocation. During the plastic deformation, the emitted dislocation from the crack tip or sources exerts back stress on the crack tip (source). The back stress is given by

$$\mathbf{s}^D = -\frac{\mathbf{mb}}{2\mathbf{pr}} \quad (2.5)$$

and the stress at the crack tip is reduced accordingly. In order to operate the source and hence continue the deformation, the applied stress must be raised.

The stress field at distance  $x$  from the crack tip when a screw dislocation is placed at distance  $r$  on a slip plane can be found readily by the method of conformal mapping [21] and is given by

$$\mathbf{s}^D = -\frac{\mathbf{mb}}{2\mathbf{p}} \left( \frac{r}{x} \right) \frac{1}{r-x} \quad (2.6)$$

Between the crack tip and dislocation ( $x < r$ ),  $\mathbf{s}^D$  is negative and thus the stress field in the vicinity of the crack tip is reduced in the presence of the dislocation. This decrease in the stress field reduces the local stress intensity factor  $k$  by a magnitude equal to [38], defined by

$$k^D = \lim_{x \rightarrow 0} \sqrt{2\mathbf{p}x} \mathbf{s}^D = -\frac{\mathbf{mb}}{\sqrt{2\mathbf{p}r}} \quad (2.7)$$

since  $k^D < 0$ , the local stress intensity  $k$  is given by

$$k = K + \sum_j^N k_j^D. \quad (2.8)$$

Thus, the local stress intensity factor is less than the applied stress intensity factor. In other words, the crack tip is shielded from the applied stress. For a dislocation at a distance  $r$  from the crack tip on a slip plane inclined to the crack plane by an angle  $\mathbf{q}$ ,  $k^D$  is given for all three loading modes by Rice and Thomson [1],

$$\begin{aligned}
k_I^D &= -\frac{3\mathbf{m}b_e}{2(1-\mathbf{n})\sqrt{2\mathbf{p}r}} \sin \mathbf{q} \cos \frac{\mathbf{q}}{2} \\
k_{II}^D &= -\frac{\mathbf{m}b_e}{2(1-\mathbf{n})\sqrt{2\mathbf{p}r}} (3 \cos \mathbf{q} - 1) \cos \frac{\mathbf{q}}{2} \\
k_{III}^D &= -\frac{\mathbf{m}b_s}{\sqrt{2\mathbf{p}r}} \cos \frac{\mathbf{q}}{2}
\end{aligned} \tag{2.9}$$

It should be noted that for  $0 < \mathbf{q} < \mathbf{p}$ ,  $k^D < 0$  for all three modes, indicating that a dislocation in these directions always shields the crack tip from the applied stress  $K$ . For  $\mathbf{p} < \mathbf{q} < 2\mathbf{p}$ , the dislocation shielding occur for mode I cracks. However, for cracks of mode II and mode III, a dislocation emitted into this region antishields the crack tip, i.e., the local  $k$  increases in the presence of dislocation. The overall effect is antishielding at a high enough applied  $K$  (below  $k_I$ ); the crack tip  $k$  exceeds  $k_{Ic}$ .

## 2.5 Model

We consider only the plane strain problem. Suppose that the crack front is contained within one slip plane, which is most highly stressed in a crystal. The slip plane makes an inclined angle  $\mathbf{q}$  with respect to the crack plane, as shown in Figure 2.1 and the crystal subjected to a pure mode I load, which includes the stress intensity factor  $K$ .

The local stress intensity factors at crack tip are given by

$$\begin{aligned}
k_I &= K + k_I^D \\
k_{II} &= k_{II}^D
\end{aligned} \tag{2.10}$$

where  $k_I^D$  and  $k_{II}^D$  are given in Equation 2.9. One can define the total local stress intensity factor at crack tip as follows:

$$k^2 = k_I^2 + k_{II}^2 \quad (2.11)$$

The local stress intensity factors along the slip plane are given by

$$K_{Islip} = \frac{1}{2} \cos\left(\frac{\mathbf{q}}{2}\right) \left[ k_I (1 + \cos \mathbf{q}) - k_{II} 3 \sin \mathbf{q} \right] \quad (2.12)$$

$$K_{IIslip} = \frac{1}{2} \cos\left(\frac{\mathbf{q}}{2}\right) \left[ k_I \sin \mathbf{q} - k_{II} (3 \cos \mathbf{q} - 1) \right]. \quad (2.13)$$

Equations 2.12 and 2.13 provide only an appropriate approximation

When the edge dislocation is emitted from the crack tip along the slip plane, the emission condition is given by Lin and Thomson [10] and Rice [11] as follows:

$$k_{II} = k_{IIe}. \quad (2.14)$$

where  $k_{IIe}$  is defined in Equation 1.4

The cleavage criterion for branching into the slip plane is given by Nuismer [39] as follows:

$$(k_I^2 + k_{II}^2) = k_{Ic}^2 \quad (2.15)$$

where  $k_{Ic}$  is the fracture toughness for the slip plane.

Suppose that the cleavage criterion is met after  $N$  dislocations are emitted. Then the local stress intensity factors at crack tip are given by

$$\begin{aligned} k_I &= K - \frac{3mb_e}{2(1-n)} \left( \sum_{j=1}^N \frac{1}{(2pr_j)^{1/2}} \right) \sin \mathbf{q} \cos \frac{\mathbf{q}}{2} \\ k_{II} &= -\frac{mb_e}{2(1-n)} \left( \sum_{j=1}^N \frac{1}{(2pr_j)^{1/2}} \right) (3 \cos \mathbf{q} - 1) \cos \frac{\mathbf{q}}{2} \end{aligned} \quad (2.16)$$

where  $r_j$  ( $j=1,2,\dots,N$ ) is the distance from the crack tip of the  $j$ th emitted dislocation.

## 2.6 Shielding by External Dislocations

Generally, external sources for dislocations exist in a material. If they are close enough to a crack tip, the stress concentration can operate them. When the crack tip collides with the dislocations generated by external sources, they may cause the crack to blunt. If the blunting is enough to arrest the crack, the fracture toughness of the material may change. Absorption of these preexisting dislocations can be enhanced by attractive elastic interaction between the crack and dislocation.

For nearby dislocations, direct interaction between the nucleating and existing dislocations cannot be represented completely by crack tip shield. Equivalently, the nucleation criteria cannot be expressed simply in terms of local stress intensity factors. Thomson [40] made some comments about the role of external dislocations in changing the overall ductile/brittle response. According to him, when a nearby source emits a dislocation in the general direction of the crack tip, the antishielding produced at the crack tip by these dislocations changes the emission/cleavage balance in the direction of greater ease of emission, and an initially sharp crack will respond by emitting a train of canceling dislocations, which will lock up the original dislocations in near the crack tip region. In this case, After the externally produced dislocations are neutralized by the emitting dislocations, the net effect of the source on the crack is shielding, which returns the emission/cleavage balance back to the cleavage side.

Lin and Thomson [41] studied the shielding provided by a single external source. They proposed that the back stress of an externally produced dislocation on the source in a stable cleavage crack is stronger than the shielding of the crack tip, because the source is closer to the dislocation pileup. Therefore, as the applied stress is raised, the cleavage criterion at the crack tip will be achieved again for a certain number of dislocations produced by the source. However, this model has not been pursued to explore the toughening properties of a discrete distribution of external sources for dislocations. However if the shape change in the crack can lower the local

$k$  below  $k_{lc}$  while external sources continue to operate, crossover to the ductile fracture mechanism is inherent in such a model,

Shastry *et al.* [42] proposed that the effect of the existing dislocations, dislocation emission on cleavage process at the crack tip, can be described in terms of a shift of the emission and cleavage surfaces in the local stress intensity space. They found that a single Volterra dislocation description shows that, in general, dislocations emitted from the crack tip tend to increase the local stress intensity required for both continuous emission on that plane and for cleavage, and they made comment that the non-local effect in the mode I crack emission would be even higher than the mode II.

Mesorovich [43] investigated direct interactions of externally generated dislocations with a moving, non-emitting crack in a BCC crystal. He pointed out that dislocation of the appropriate Burgers vector, initially residing in a strip ahead of the inter coming crack tip, were strongly attracted to and funneled toward the crack tip, with motion of each being restricted to its own slip plane. Once drawn into the vicinity of the tip, these dislocations inevitably caused local, atomic scale blunting of the tip.

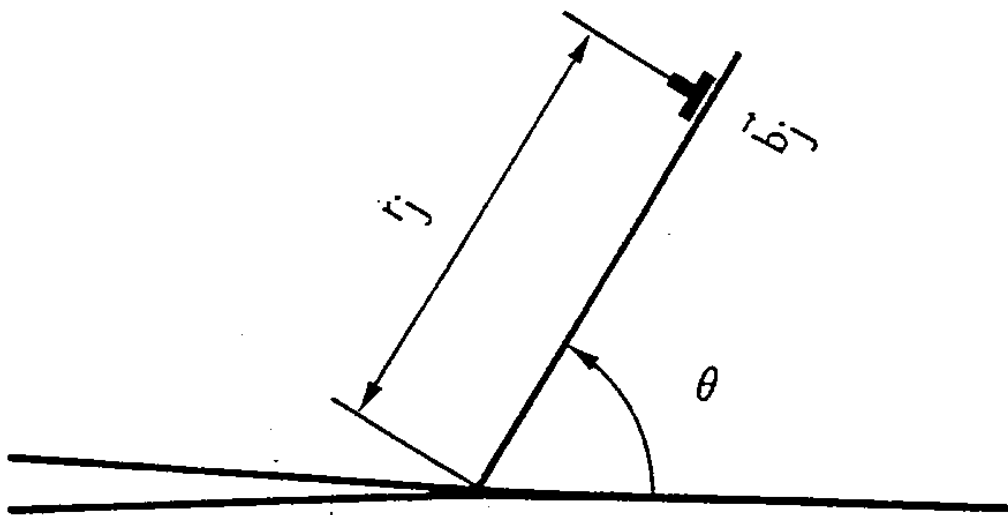


**Figure 2.1** Coordinate system for a crack and an emitted dislocation.

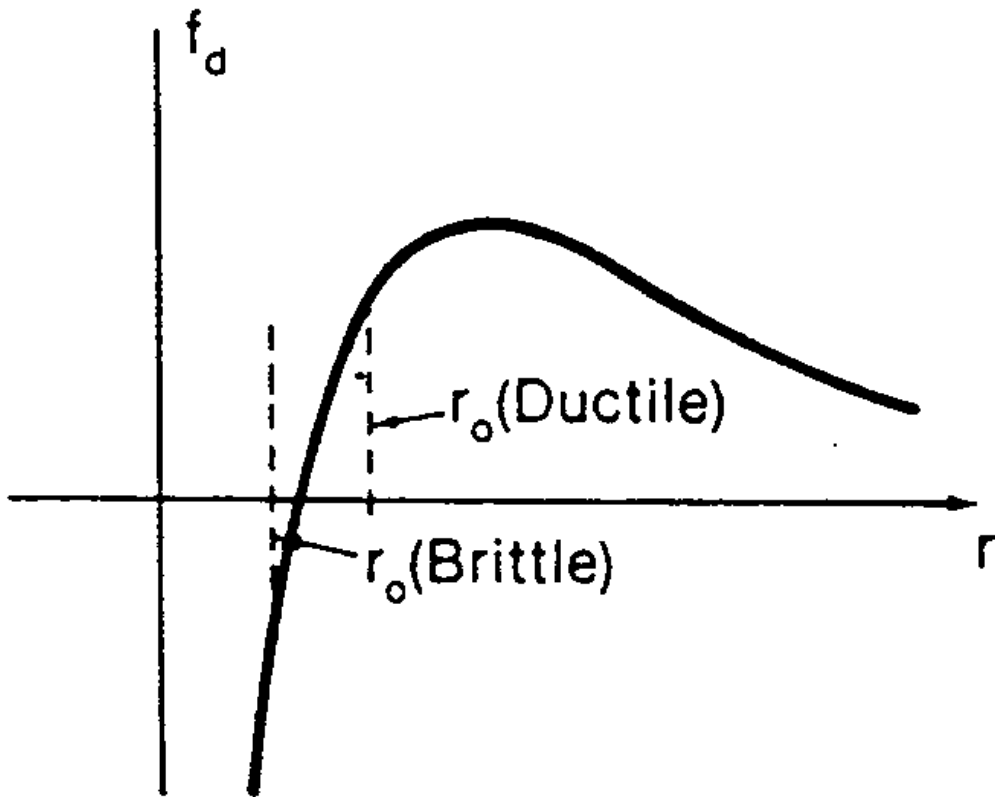


**Figure 2.2** Force on a dislocation in the vicinity of a crack [27].

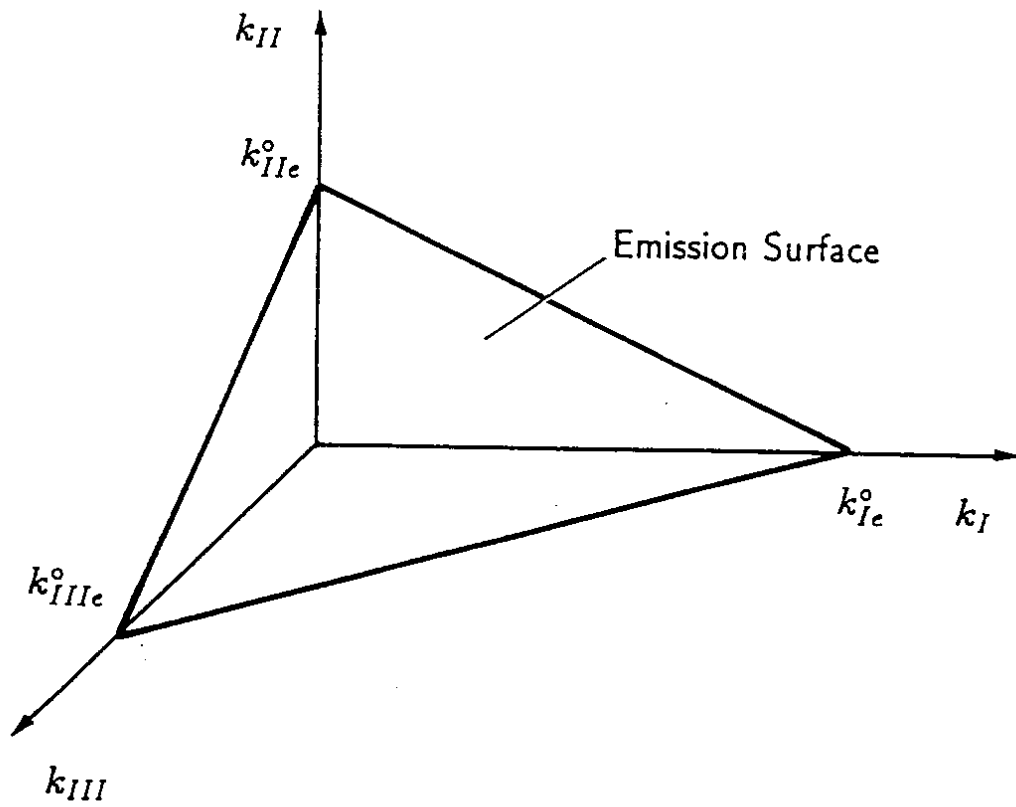


**Figure 2.3** Emission surface in k-space [23].

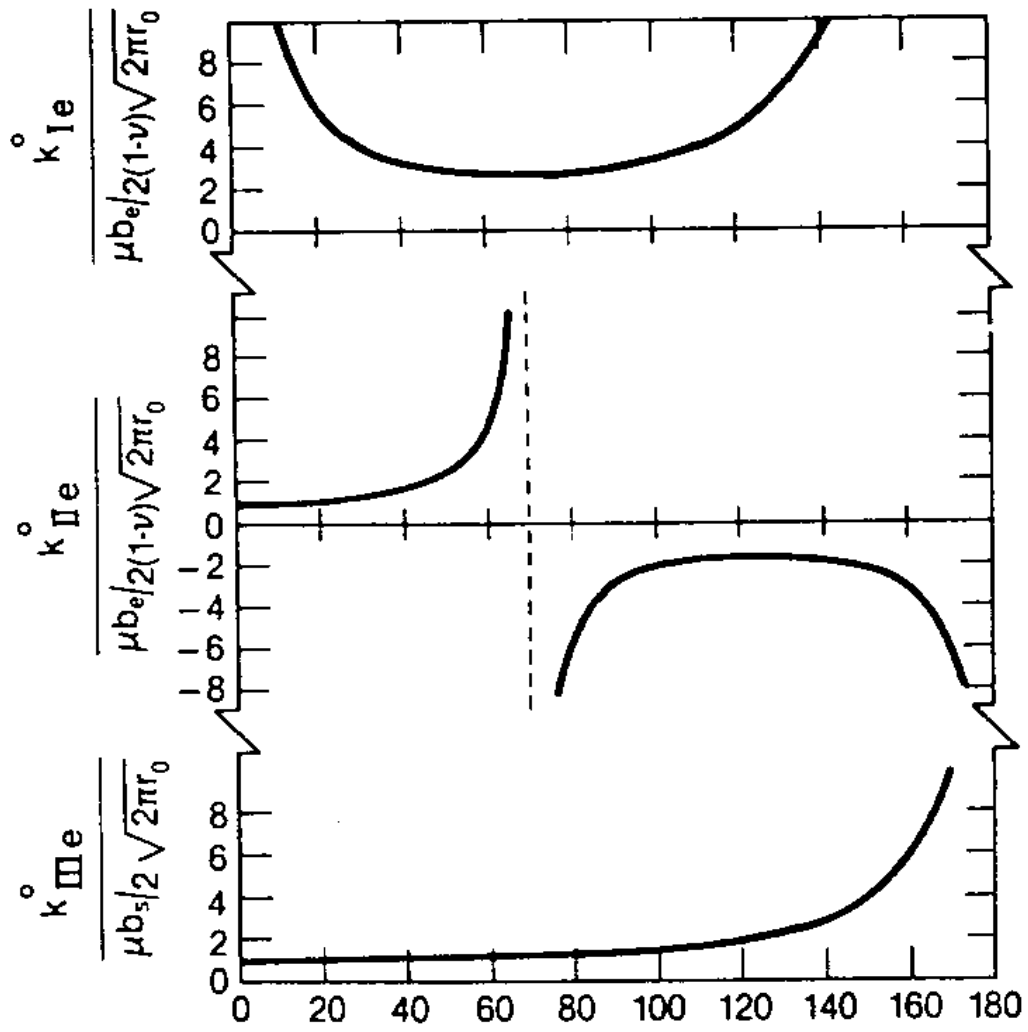


Figure 2.4 Angular plots for  $k_{ie}^0$  [23].

# Chapter 3

## Atomistic Simulation of Fracture

### 3.1 Introduction

The use of atomistic simulation methods is becoming increasingly common in material science. Simulations are being designed that more and more closely approximate real materials systems and processes since computer speeds continue to increase.

Experiments give the general behavior of a material when subjected to different conditions. However, it is difficult to observe experimentally the behavior of atoms and their dynamics. The computer simulation, therefore, becomes the appropriate tool, and it is possible to simulate what happens on the atomic scale, and hence to compare with the results obtained by experiments.

Computer simulations of fracture that deal entirely with the atomic interactions and displacements at crack tip provide a very useful supplement to elastic and elastic/plastic analyses. The utility of these calculations is that they provide a fairly simple way for examining in great detail the atomic configuration of a crack tip, or other defect, by molecular dynamics or molecular statics technique approach using interatomic forces.

The molecular statics technique is very simple. When it is combined with the conjugate gradient method, it allows very fast relaxation. Because of this advantage, the method can be applied to large systems up to  $10^8$  atoms. However, the static relaxation gives the structure of defect at zero temperature, and hence thermal expansion, atomic

vibration etc. are neglected. These temperature effects are accomplished by molecular dynamics (MD).

The properties predicted by an atomistic simulation are only as good as the quantity of the underlying interatomic potential. The Embedded Atom Method (EAM), is a recently developed form of interatomic potential that has lead to considerable improvement in the quality of prediction for metals and intermetallics. However, it fails in the cases where the Cauchy relation for metal or alloy is negative, and for covalent materials.

### 3.2 The Embedded -Atom Method

The EAM is a simple procedure for computing the electronic contribution to cohesion in metals. The EAM, a semi-empirical method, is based on the Hohenber-Kohn theorem [44], which states that the energy contribution of an atom in an array of interacting atoms is a function of the local electron density, due to all other atoms. A periodic array of atoms is not required in the EAM. Consequently, it can be used for disordered alloys, surfaces, cracks, dislocation cores, grain boundaries, stacking faults, and liquid -solid phase interfaces.

Within the EAM approach [2,3], the total energy of the system is defined as the sum of two contributions; the interaction energy of each atom with the local electron density associated with neighboring atoms within a selected cut -off distance, called the *embedded energy*, and the pair interaction energy mimicking the electrostatic interaction between the atoms. Consequently, the total potential energy  $E_{tot}$  is written as

$$E_{tot} = \sum_i F_i(\mathbf{r}_i) + \frac{1}{2} \sum_{i,j(i \neq j)} \mathbf{f}_{ij}(R_{ij}) \quad (3.1)$$

where  $F_i$  is the embedded energy density at the position of atom  $i$ ,  $\mathbf{r}_i$  is the total electron density at the position of atom  $i$ , and  $\mathbf{f}_{ij}(R_{ij})$  is the pair interaction between atom  $i$  and  $j$  separated by the distance  $R_{ij}$ . The electron density at each site is computed from the superposition of spherically averaged atomic electron density as

$$\mathbf{r}_i = \sum_{j \neq i} \mathbf{r}_j^a(R_{ij}) \quad (3.2)$$

where  $\mathbf{r}_j^a(R_{ij})$  is the atomic electron density at a distance  $R_{ij}$  from the nucleus of atom  $j$ . The superscript  $\mathbf{a}$  in  $\mathbf{r}_j^a(R_{ij})$  is used to specify the species of atom  $j$ . The summations in Equations 3.1 and 3.2 are carried out over all the neighboring atoms of a given atom within the selected cut-off distance.

The embedding energies and pair interactions are generally determined by fitting various physical quantities of a system, such as the sublimation energy, the lattice constants, the second order elastic constants, the formation energy of various defect and zero temperature of [45]. Once the embedding and the pair interactions functions are determined, the total potential energy of a metallic material in the given structure can be calculated from the (3.1).

Interatomic potential for aluminum developed by Mishin *et al.* [46] is used in this study. The potential is fitted the experimental values of the lattice parameter, the atomic volume, cohesive energy and the elastic constants.

### 3.3 Interatomic Potential

The EAM potential used to describe the interatomic interaction in aluminum is fitted to the experimental values of the lattice parameter, the atomic volume, cohesive energy, the unrelaxed vacancy formation energy, and the elastic constants. In the particular cohesive energy  $E_{coh} = 3.36 \text{ eV}$ , the vacancy formation energy  $E_v = 0.68 \text{ eV}$ , the lattice parameter  $a = 4.05 \text{ \AA}$  and the elastic constant  $c_{11} = 0.712 \text{ eV/\AA}^3$ ,  $c_{12} = 0.386 \text{ eV/\AA}^3$  and  $c_{44} = 0.197 \text{ eV/\AA}^3$ . The atomic volume is  $16.60 \text{ \AA}^3$ .

The cut of radius atomic interaction is  $6.2872 \text{ \AA}$  and the interactions of all atoms with separation greater than this cut off distance is set to zero. The minimum allowed distance between the atoms is  $1 \text{ \AA}$ . The surface energy calculated from this potential for

the (111) plane is equal to  $0.056\text{eV}/\text{\AA}^2$ , and unstable stacking fault energy for the  $[112](1\bar{1}\bar{1})$  slip system is  $0.00995\text{eV}/\text{\AA}^2$ .

### 3.4 Simulation Technique

It is necessary for atomistic simulations to correctly formulate boundary conditions such that the size is optimized for minimum computational time without allowing the artificial perturbation of the defect by boundary conditions.

In this study, we use a molecular statics technique for the atomistic simulation. Using the molecular statics technique with the EAM potential, it is possible to address questions about the relative stabilities and structures of aluminum. Molecular statics refers to the procedure of finding the atomic geometry that corresponds to the lowest energy for a given defect specification. These energies and structures thus correspond to the classical zero-temperature system, representing a good approximation at low temperatures. If accurate results are desired for a specific non-zero temperature, Metropolis Monte Carlo [47] or molecular dynamics can be employed to the study of the appropriate constant temperature ensemble.

For the simulation, the first step is the generation of the perfect lattice based upon information of the Bravais lattice of the material and repeating this along the Cartesian coordinates. The lattice parameters determine the length of the orthogonal vectors. Then an elliptical crack is introduced in the lattice as shown in Figure 3.1. After the defect introduction, the boundary conditions are imposed. The periodic boundary condition is used in the z-direction so that the crack is effectively of infinite length and the plane of atoms in the x and y-direction are fixed except for the surface where the crack is introduced. To simulate a uniaxial tension, a force is applied in the y-direction by displacing the fixed atoms at the surface according to the anisotropic elastic solution for a stressed solid.

This computational block (Figure 3.1) consists of two parts, Region I and Region II: Region I includes the crack, and it contains the atoms which are entirely free to move according to the interactions defined by the potentials and do so to minimize the energy of the crystal. Region II contains the atoms that are fixed on normal lattice sites and influenced by the long-range elastic interactions of the defect. These atoms interact with neighboring atoms in Region I, but their coordinates do not change.

Energy minimization of Region I is accomplished by the application of the conjugate gradient technique [48]. This minimization technique moves the atoms from their initial position towards the direction with the steepest gradient, i.e., the direction in which the rate of energy decrease is a minimum. This movement occurs until the energy gradient is zero. On obtaining the lowest energy position, the process of atom movement in a perpendicular direction occurs. This iteration procedure continues until no further decrease in energy is possible by movement in a perpendicular direction. The total energy of the blocks is determined by considering all possible pairs within the cut-off radius of the potential.

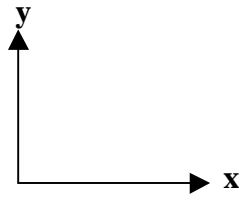
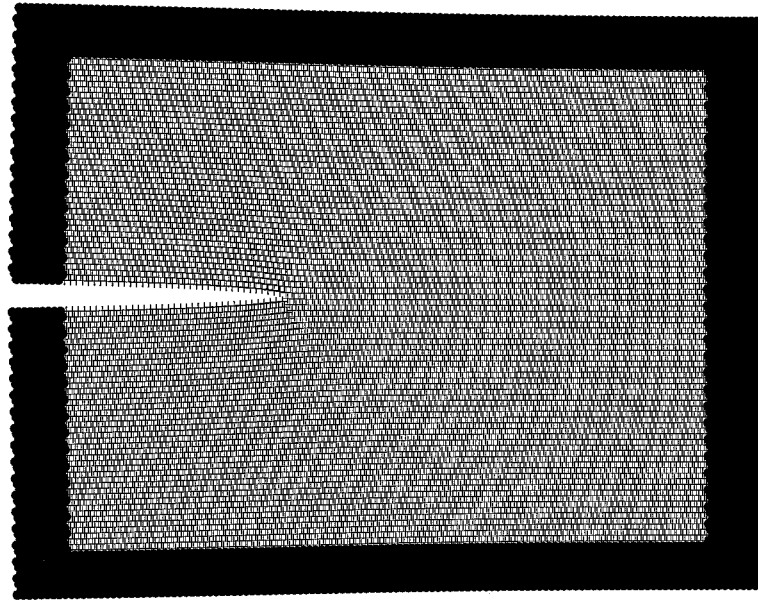


**Figure 3.1** A computational block. The black part represents the fixed boundary region.

# Chapter 4

## Simulation Results

### 4.1 Introduction

In this study, a molecular statics technique with the EAM potential developed for aluminum by Mishin *et al.* [46] was used. The cut-off radius of atomic interaction is 6.2872 Angstrom ( $A^\circ$ ), and the minimum allowed distance between the atoms is  $1A^\circ$ . Edge vectors of the simulation blocks are  $[11\bar{2}][111]$  and  $[\bar{1}\bar{1}0]$ .

Nine different sizes of the blocks were used such as 2000, 5000, 10000, 18000, 33000, 64000, 92000, 180000 and 400000 atoms. A crack is produced in each block at a position of  $x=0.1A^\circ$  and  $y=0.1A^\circ$ , lying on the x-y plane. The cracks are on (111) plane, and their front is along  $[\bar{1}\bar{1}0]$  direction. All the blocks are subjected to the same deformation process. That is, the simulation blocks are subjected to a pure mode I load. The loading is started at  $0.15 eV(\bar{A})^{-2.5}$ , which is lower than the Griffith value,  $0.239 eV(\bar{A})^{-2.5}$  obtained from Equation 1.3, and the loading is increased in intervals of  $0.025 eV(\bar{A})^{-2.5}$  until the crack tip cleaves.

As the applied stress intensity factor is raised, the total local stress intensity factor  $k$  at the crack tip increases. The manner in which the crack grows will depend on whether  $k$  reaches  $k_{IIe}$  or  $k_{Ic}$  first. The blocks, in the present study, resume dislocation

emission as the cracks are loaded since the critical stress intensity factor for dislocation emission,  $0.07 \text{ eV}(\text{Å})^{-2.5}$  according to emission criterion by Rice [23], is less than that for crack propagation,  $0.239 \text{ eV}(\text{Å})^{-2.5}$  from the Griffith relation. Therefore, the blocks will fail in a ductile manner.

For all cases, the first continuous edge dislocation with Burgers vector  $1/6[112]$  is emitted from the crack tip due to the plastic deformation when the applied stress intensity factor reaches  $0.2 \text{ eV}(\text{Å})^{-2.5}$ , i.e., the stress on the dislocation from the crack tip field exceeds the image stress. Since the net force on it is positive, it travels away from the crack tip until the force is equal to the lattice friction force. The emission occurs along  $[112]$  slip direction inclined at an angle of  $70.5^\circ$  with respect to the crack tip as shown in Figure 4.1 (a) and (a'). As the applied stress intensity factor is raised, more dislocations are generated from the crack tip along the same direction. The emitted dislocations are Shockley partial (imperfect) dislocations creating stacking faults as they move away from the crack tip. Zhou *et al.*[49] and Hoagland *et al.*[50] have shown that emission of the partial dislocations is observed for various orientations in FCC metals. However, even in ductile materials, dislocations are not emitted in geometries where a slip plane is not available. The purely brittle behavior of the crack tip observed in these cases is due to the periodic boundary condition imposed parallel to the crack front. On the other hand, Bacquart [51] has shown that aluminum is a very ductile material in which the cracks do not propagate, and the cracks are blunted by the emitted partial dislocations if the periodic boundary condition is not imposed parallel to the crack front.

All of the emitted dislocations have identical Burgers vectors, and they lie on the parallel  $(1\bar{1}1)$  slip planes, which produce overlapping stacking faults on these planes. The overlapping stacking faults form a twin as shown in Figure 4.1.

The emitted dislocations intersect the crack front, and the Burgers vector  $1/6[112]$  has a component normal to the crack plane. This agrees well with Rice and Thomson's requirement of blunting of a mode I crack.

Cottrell [52] suggested that crack tip blunting could result from the emission of edge dislocations on planes inclined at  $45^{\circ}$  to the crack. In the present study, the cracks emit the partial dislocations on  $(11\bar{1})$  slip planes inclined at an angle of  $70.5^{\circ}$  to the crack tip in aluminum during the loading of the mode I crack. When the first dislocation is nucleated from the crack tip, the crack is blunted. After the second dislocation is generated, the geometry of the crack is shaped as a blunted crack with a sharp corner because the dislocations are emitted on one side of the crack as shown in Figure 4.1. Furthermore, the emission of further dislocations does not change the shape of the blunted crack.

Rice and Thomson derived the critical distance at which the stress on a dislocation vanishes. It was proposed that, if this critical distance was less than the core radius of the dislocation, dislocation emission would occur and blunt the crack. Using this criterion, most FCC metals including aluminum are expected to generate dislocation spontaneously from the crack tip. Therefore, their prediction is in agreement with our simulation in aluminum that arrested mode I cracks are always blunted by emitting edge dislocation. The crack tip blunting processes are important, because an increase in the fracture toughness may result from the blunting.

The dislocation density is extended to be very high near the crack tip and decreases gradually away from the crack tip. Therefore, the dislocations are in the form of an inverse pileup [33]. On the other hand, in situ Transmission Electron Microscopy (TEM) observations of dislocation emission at a crack tip in aluminum [53] do not agree with this result.

The emitted dislocations shield the crack tip from the applied  $K$ . Furthermore, although pure mode I loading is applied on the blocks, the dislocations generated from the crack tip introduce a mode II local stress intensity factor  $k_{II}^D$ . The calculation of the local stress intensity factors is carried out using Equation 2.9. For this specific inclined

angle  $\mathbf{q} = 70.5^\circ$ , which is the angle of maximum shear stress for a mode I crack (Stroh's condition [54]),  $k_{II}^D$  is nearly equal to zero.

After a certain number of dislocations are nucleated from the crack tip, the emission stops because of the strong shielding. This is followed by the brittle propagation without the cracks branching in the blocks as shown in Figure 4.1 (g) and (g'). After the cracks propagate forward a short distance, they are blunted again by the dislocations emitted on the parallel planes (Figure 4.1 (g) and (g')).

It is clear that dislocation emission is initially favored, but there is a cleavage transition for a critical number of emitted dislocations. As the cracks cleave, some dislocations, especially the last emitted ones, which are closer to the crack tip, come towards to the crack tip (Figure 4.1 (g) and (g')), and such behavior has also been obtained experimentally by Zhang *et al.* [55].

## 4.2 Twin Formation

Under high loading rates or at low temperatures, twinning is a preferred mode of deformation in BCC metals. Although it is possible in FCC metals, it is not common at high temperatures, or even at room temperature in pure metals such as Nickel (Ni) and aluminum. Some FCC lattices are found to twin upon tensile experiments at a very low temperature  $4.2 \text{ } ^\circ K$  under specific orientation conditions with a strain rate between  $10^{-5}$  and  $10^{-4} \text{ s}^{-1}$ , under a high level of stress (such as copper (Cu) [56] and nickel (Ni) [57]). However, twinning has not been observed in aluminum under experimental conditions similar to those applied to copper and nickel. This is because of the large value of stacking fault energy in aluminum. Aluminum [53], nickel [58], and copper [59] have also been studied using the in situ TEM technique. Twinning has been observed in nickel and copper because of the high deformation rate and high stress concentration at the crack tip, but it has not been observed in aluminum, again due to the high stacking fault. It is agreed that the lower the stacking fault, the higher the

probability of twin formation in a metal. Aluminum, which has high stacking energy, does not twin easily. Twinning, however, was observed ahead of the cracks during the present simulation. Probably the low temperature facilitates twin formation. Also, twinning was observed with high strain rate ( $\sim 10^9 s^{-1}$ ) in the simulation of aluminum [51].

Since the twin formation is energetically more favorable than the formation of an irregularly shaped stacking fault, the fault is most likely a thin twin formed by overlapping stacking faults on successive planes. Extended dislocation lying in the region adjacent to the twin boundary increases the thickness of the twin by one layer. Once a twin is formed, it can grow more easily because of the reduction of the stacking fault energy in the vicinity of the twin boundary.

### 4.3 Geometry of the Crack Tip

The dislocations generated by plastic deformation change the geometry of the crack tip. A mode I crack is often blunted by emitting dislocations on inclined planes [1,21,22]. The Rice and Thomson model [1] requires two conditions for blunting of mode I cracks: firstly, the Burgers vector must have a component normal to the crack plane and secondly, the slip plane must intersect the crack front along its whole length. These are the stringent restrictions on the crack geometry. In the present study, both of the conditions are satisfied.

The shape of a crack is crucial to its behavior, because if the shape is rounded instead of being sharp, then no stress singularity exists at the crack tip. In that case, the stress concentration is generally not large enough to break bonds at the crack tip, even though it may be sufficient to generate plasticity in the material surrounding the crack.

Probably the main method of modifying the shape of a crack is through dislocation emission. When dislocations are progressively emitted from the crack tip first on one side of the crack and then on the other side, a sharp crack changes into a

wedge crack. The sharp corner of a wedge tip does not involve an elastic singularity as strong as a slit crack [60].

Experiments [29,61] indicate that under mode I loading conditions, dislocations are generated along at least two inclined slip planes that are symmetric with respect to the crack plane. However, in the present study, the dislocations are emitted on one side only because of the crystallographic orientation. Since the (111) plane is not a mirror plane, there is only one slip plane. The result obtained is in agreement with the experiment made in aluminum by Horton and Ohr [53]. They studied in situ TEM observations of dislocation emission at a crack tip in aluminum, and they found that the dislocations were generated along one side of the crack, and the crack was blunted.

After the emission of the first dislocation, the crack is blunted (Figure 4.1 (a) and (a')). As the second dislocation is generated, the geometry of the crack becomes blunted with a sharp corner (Figure 4.1) because of the asymmetric emission of the dislocations, i.e., the dislocations are generated on one side only. The crack tip stays at the same layer as shown in Figure 4.1. Therefore, the emission of further dislocations maintains the geometry of the crack until the crack cleaves. Probably, if the dislocations had been nucleated symmetrically, the geometry of the crack would have been a wedge crack. Such sharp corner geometry has been studied by using a hexagonal two-dimensional atomistic model by Schiotz *et al.* [62,63]. The presence of the sharp corners in the blunted cracks is highly significant to their behavior, because the stress concentrations appear at these corners and may be almost as strong as the stress concentration of a sharp crack tip. The sharp corner preserves the stress concentration, reducing the effect of the blunting [63].

Macroscopically blunted cracks may appear to have a smooth shape, but when the blunting is only a few tens of lattice constants, or even smaller, the crystal structure makes it almost inevitable for sharp corners to be present in the crack tip configuration. Furthermore, the dislocation emission process creating the blunting almost leads to angular crack tip shapes and does not create a smoothly blunted crack.